

# Integral boundary conditions in phase field models

Xiaofeng Xu<sup>a</sup>, Lian Zhang<sup>a</sup>, Yin Shi<sup>b</sup>, Long-Qing Chen<sup>b</sup>, Jinchao Xu<sup>1a</sup>

<sup>a</sup>Department of Mathematics, Pennsylvania State University, University Park, PA, 16802, USA

<sup>b</sup>Department of Material Science and Engineering, Pennsylvania State University, University Park, PA, 16802, USA

---

## Abstract

Modeling the microstructure evolution of a material embedded in a device often involves integral boundary conditions. Here we propose a modified Nitsche's method to solve the Poisson equation with an integral boundary condition, which is coupled to phase-field equations of the microstructure evolution of a strongly correlated material undergoing metal-insulator transitions. Our numerical experiments demonstrate that the proposed method achieves optimal convergence rate while the rate of convergence of the conventional Lagrange multiplier method is not optimal. Furthermore, the linear system derived from the modified Nitsche's method can be solved by an iterative solver with algebraic multigrid preconditioning. The modified Nitsche's method can be applied to other physical boundary conditions mathematically similar to this electric integral boundary condition.

*Keywords:* Phase field, Integral boundary condition, Lagrange multiplier method, Modified Nitsche's method, Algebraic multigrid.

---

## 1. Introduction

Many physical processes may be controlled by external constraints corresponding to complex boundary conditions in their theoretical models other than the standard Neumann, Dirichlet, or Robin boundary conditions. For example, in the electrically induced insulator-metal transitions [1, 2, 3, 4, 5, 6, 7], the phase-changing material is often in series connection to a resistor, so a type of integral boundary condition naturally arises. The series resistor can protect the material from large current damage, and sometimes is even crucial for the emergence of desired phenomena such as the voltage oscillation in vanadium dioxide [1, 2, 3] and the chaotic dynamics in niobium dioxide Mott memristors [6, 7]. This form of integral boundary condition may also arise in other physical processes. For example, one may encounter a scenario in which a material is in a finite thermal bath and they as a whole are isolated. These imply that the surface temperature of the material is uniform, and is determined by the energy conservation of the total energy of the material and thermal bath. The boundary condition on the surface  $S$  of the material is then  $C_b \partial T / \partial t = - \int_S k (\partial T / \partial n) dA$ , where  $C_b$  is the heat capacitance of the thermal bath,  $T$  is the temperature on  $S$ ,  $t$  is the time, and  $k$  is the thermal conductivity of the material. In this paper, we discuss ways of handling such a special type of integral boundary condition encountered in many electric circuit systems. This boundary condition is illustrated by the typical circuit shown in Figure 1, in which a material of interest is electrically excited by a direct voltage source  $V$  through a series resistor  $R$ . We consider the material to be two-dimensional, that is, the material has uniform properties along the third dimension (out of plane). The thickness in the third dimension is set to 1. The length and width are both  $L$ . The physical partial differential equation (PDE) determining the electric potential field  $\Phi(x, y)$  in the material is given by Gauss's law with proper boundary conditions,

$$\begin{cases} -\Delta\Phi(x, y) = f(x, y) & \text{in } \Omega = (0, L)^2, \\ \Phi = V - IR & \text{on } \Gamma_1 = \{(x, y) \in \partial\Omega : x = 0\}, \\ \frac{\partial\Phi}{\partial y} = 0 & \text{on } \Gamma_2 = \{(x, y) \in \partial\Omega : y = 0 \text{ or } L\}, \\ \Phi = \Phi_D & \text{on } \Gamma_3 = \{(x, y) \in \partial\Omega : x = L\}, \end{cases} \quad (1.1)$$

where  $(x, y)$  denote the spatial coordinates,  $I$  is the current passing through the boundary  $\Gamma_1$ ,  $\Phi_D$  is the fixed potential at the boundary  $\Gamma_3$ , and the source term  $f(x, y)$  depends on the charge distribution inside the material. The special boundary condition arises at the boundary  $\Gamma_1$ . The value of  $\Phi$  on  $\Gamma_1$  is determined by Kirchhoff's law and Ohm's law, that is, it is the difference between the total voltage  $V$  and the voltage drop across the resistor,  $IR$ . We denote the

---

<sup>1</sup>Corresponding author: xu@math.psu.edu (Jinchao Xu)

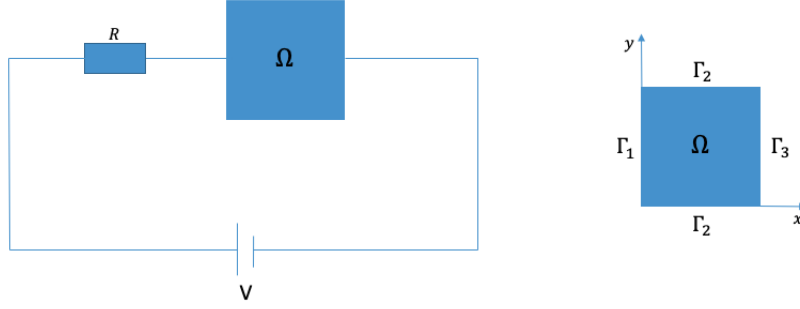


Figure 1: A simple model

area and the outward unit normal vector of the boundary  $\Gamma_1$  by  $S = \Gamma_1 \times [0, 1]$  and  $\mathbf{n}$ , respectively. The current  $I$  is related to the current density  $\mathbf{J} = -\sigma \nabla \Phi$  (Ohm's law,  $\sigma$  is the conductivity of the material) through the following surface integral:

$$I = - \int_S \mathbf{J} \cdot \mathbf{n} dA \quad (1.2)$$

$$= \int_{\Gamma_1} \sigma \frac{\partial \Phi}{\partial n} ds. \quad (1.3)$$

The negative sign in the first equality arises since the current flows into the material across  $\Gamma_1$ . Finally, we obtain the following integral boundary condition at  $\Gamma_1$ :

$$\Phi = V - R \int_{\Gamma_1} \sigma \frac{\partial \Phi}{\partial n} ds. \quad (1.4)$$

The equipotential on  $\Gamma_1$  is determined by an integral of its gradient over that boundary.

In formulating the variational problem for PDEs with such complex integral boundary conditions, and solving it by the finite element method, one difficulty is that these boundary conditions cannot be easily incorporated into the weak form like a Neumann or Robin boundary condition, or enforced on the boundaries like a Dirichlet boundary condition. Therefore, we have to develop special methods to deal with this kind of special boundary condition. A general way of handling a special boundary condition is to treat it as a constraint for the PDE, and then use the Lagrange multiplier method to convert the PDE problem to a stationary point problem. An example of treating a Dirichlet boundary condition using Lagrange multiplier method can be found in [8, 9]. Another widely used method is to add a penalty term such as the Nitsche's method [10, 11]. In this paper, we propose a modified Nitsche's method to handle the integral boundary condition (1.4) in solving the PDE (1.1) by the finite element method.

The paper is organized as follows. In Section 2, we formulate the variational problem using the Lagrange multiplier method, then we propose a modified Nitsche's method that allows us to incorporate the special boundary condition into the variational form naturally. Numerical tests are presented in Section 3. The results show that our proposed method achieves better accuracy than the Lagrange multiplier method, and the resulting linear system can be efficiently solved by an iterative solver with algebraic multigrid (AMG) preconditioning. Finally we come to a conclusion in Section 4.

## 2. Methods

In this section, we briefly review the Lagrange multiplier method and then propose a new method to solve problem (1.1) with boundary condition (1.4), based on Nitsche's method. In order to derive the variational form of the two methods, we define the following function spaces:

$$V_\Phi = \{ \Phi \in H^1(\Omega) \mid \Phi|_{\Gamma_3} = \Phi_D \}, \quad (2.1)$$

$$V_{\Phi,0} = \{ \Phi \in H^1(\Omega) \mid \Phi|_{\Gamma_3} = 0 \}, \quad (2.2)$$

$$V_\lambda = L^2(\Gamma_1), \quad (2.3)$$

where  $L^2(\Gamma_1) = \{ \Phi : \Gamma_1 \rightarrow \mathbb{R} \mid \int_{\Gamma_1} \Phi^2 dx < \infty \}$ , and  $H^1(\Omega) = \{ \Phi \in L^2(\Omega) \mid \int_{\Omega} |\nabla \Phi|^2 dx < \infty \}$ .

For the space discretization, we use a uniform triangular mesh  $\mathcal{T}^h$  of the domain  $\Omega$ , where  $h$  denotes the mesh size of  $\mathcal{T}^h$ . We let  $V_\Phi^h, V_{\Phi,0}^h, V_\lambda^h$  be the standard finite element subspaces of  $V_\Phi, V_{\Phi,0}, V_\lambda$  defined as follows,

$$V_{\Phi}^h = \{ \Phi_h \in C(\bar{\Omega}) \cap V_{\Phi} \mid \Phi_h|_{\mathcal{K}} \in P_n(\mathcal{K}), \forall \mathcal{K} \in \mathcal{T}^h \}, \quad (2.4)$$

$$V_{\Phi,0}^h = \{ \Phi_h \in C(\bar{\Omega}) \cap V_{\Phi,0} \mid \Phi_h|_{\mathcal{K}} \in P_n(\mathcal{K}), \forall \mathcal{K} \in \mathcal{T}^h \}, \quad (2.5)$$

$$V_{\lambda}^h = \{ \lambda_h \in C(\Gamma_1) \mid \lambda_h|_{\mathcal{K} \cap \Gamma_1} \in P_n(\mathcal{K} \cap \Gamma_1), \forall \mathcal{K} \in \mathcal{T}^h \}, \quad (2.6)$$

where  $P_n(\mathcal{K})$  is the space of polynomials of degree at most  $n$  on  $\mathcal{K} \in \mathcal{T}^h$ , with  $n \geq 1$ . In our numerical tests, we use continuous piecewise linear functions for the finite element space, i.e.  $n = 1$ .

### 2.1. Lagrange multiplier method

In this subsection, we use the Lagrange multiplier method to solve equation (1.1) with integral boundary condition (1.4) on  $\Gamma_1$ . By this method [12], solving equation (1.1) with (1.4) is equivalent to finding the stationary point of the following functional

$$\int_{\Omega} \left( \frac{1}{2} |\nabla \Phi|^2 - f \Phi \right) dx - \int_{\Gamma_1} \lambda \left( V - \Phi - R \int_{\Gamma_1} \sigma \frac{\partial \Phi}{\partial n} ds \right) ds, \quad (2.7)$$

where  $\Phi \in V_{\Phi}$ , and  $\lambda \in V_{\lambda}$  is the Lagrange multiplier. Based on the functional (2.7), we introduce the following bilinear form

$$\begin{aligned} B(\Phi, \lambda; v_1, v_2) &= \int_{\Omega} \nabla \Phi \cdot \nabla v_1 dx + \int_{\Gamma_1} \lambda v_1 ds \\ &\quad + R \int_{\Gamma_1} \lambda \left( \int_{\Gamma_1} \sigma \frac{\partial v_1}{\partial n} ds \right) ds + \int_{\Gamma_1} \Phi v_2 ds + R \int_{\Gamma_1} \left( \int_{\Gamma_1} \sigma \frac{\partial \Phi}{\partial n} ds \right) v_2 ds, \end{aligned} \quad (2.8)$$

and a functional

$$F(v_1, v_2) = \int_{\Omega} f v_1 dx + V \int_{\Gamma_1} v_2 ds, \quad (2.9)$$

where  $v_1 \in V_{\Phi,0}$ , and  $v_2 \in V_{\lambda}$ .

The stationary point  $(\Phi, \lambda) \in V_{\Phi} \times V_{\lambda}$  of (2.7) is such that for all  $v_1 \in V_{\Phi,0}$ ,  $v_2 \in V_{\lambda}$ ,

$$B(\Phi, \lambda; v_1, v_2) = F(v_1, v_2). \quad (2.10)$$

The corresponding finite element formulation is shown in Algorithm 1.

---

#### Algorithm 1: FEM with Lagrange multiplier method

---

Find  $\Phi_h \in V_{\Phi}^h$ ,  $\lambda_h \in V_{\lambda}^h$  such that for all  $v_{1,h} \in V_{\Phi,0}^h$ ,  $v_{2,h} \in V_{\lambda}^h$ ,

$$B(\Phi_h, \lambda_h; v_{1,h}, v_{2,h}) = F(v_{1,h}, v_{2,h}). \quad (2.11)$$


---

### 2.2. Modified Nitsche's method

In the Lagrange multiplier method (2.11), an additional variable  $\lambda_h$  is introduced. We also note that in the bilinear form of (2.11), there are derivative terms in the integrals, which might lead to convergence problems. Here we propose a modified Nitsche's method to handle these issues. This proposed method does not require an additional Lagrange multiplier variable, and the resulting boundary condition does not involve a derivative term in the integral.

We assume that  $\sigma$  is always positive, i.e.  $\sigma : [0, L] \rightarrow \mathbb{R}^+$ , which is true in most physical situations. By introducing a small term  $\epsilon \frac{\partial \Phi}{\partial n}$  with a small positive fine-tuned constant  $\epsilon$ , we replace the boundary condition (1.4) by the following

$$\Phi + \epsilon \frac{\partial \Phi}{\partial n} = V - R \int_{\Gamma_1} \sigma \frac{\partial \Phi}{\partial n} ds. \quad (2.12)$$

Using (2.12) directly as a boundary condition is the classic Nitsche's method [10]. Multiplying  $\sigma$  on both sides of equation (2.12), we have

$$\sigma \Phi + \epsilon \sigma \frac{\partial \Phi}{\partial n} = \sigma V - R \sigma \int_{\Gamma_1} \sigma \frac{\partial \Phi}{\partial n} ds. \quad (2.13)$$

Integrating both sides of equation (2.13) over  $\Gamma_1$  and rearranging the equation, we obtain

$$\int_{\Gamma_1} \sigma \frac{\partial \Phi}{\partial n} ds = \frac{1}{R \int_{\Gamma_1} \sigma ds + \epsilon} \int_{\Gamma_1} (\sigma V - \sigma \Phi) ds. \quad (2.14)$$

Substituting equation (2.14) into equation (2.12) gives

$$\Phi + \epsilon \frac{\partial \Phi}{\partial n} = V - \frac{R}{R \int_{\Gamma_1} \sigma ds + \epsilon} \int_{\Gamma_1} (\sigma V - \sigma \Phi) dy. \quad (2.15)$$

Rearranging equation (2.15), we obtain the boundary condition on  $\Gamma_1$  for problem (1.1)

$$\frac{\partial \Phi}{\partial n} = \frac{1}{\epsilon} \left( V - \Phi - \frac{R}{R \int_{\Gamma_1} \sigma ds + \epsilon} \int_{\Gamma_1} \sigma V ds + \frac{R}{R \int_{\Gamma_1} \sigma ds + \epsilon} \int_{\Gamma_1} \sigma \Phi ds \right), \quad (2.16)$$

which can be implemented like a Neumann boundary condition.

We introduce the following bilinear form

$$a(\Phi, v_1) = \int_{\Omega} \nabla \Phi \cdot \nabla v_1 dx + \frac{1}{\epsilon} \int_{\Gamma_1} \left( \Phi - \frac{R}{R \int_{\Gamma_1} \sigma ds + \epsilon} \int_{\Gamma_1} \sigma \Phi ds \right) v_1 ds, \quad (2.17)$$

and a functional

$$L(v_1) = \int_{\Omega} f v_1 dx + \frac{1}{\epsilon} \int_{\Gamma_1} \left( V - \frac{R}{R \int_{\Gamma_1} \sigma ds + \epsilon} \int_{\Gamma_1} \sigma V ds \right) v_1 ds. \quad (2.18)$$

Now the variational problem reads as follows: find  $\Phi \in V_{\Phi}$ , for all  $v_1 \in V_{\Phi,0}$ , such that

$$a(\Phi, v_1) = L(v_1). \quad (2.19)$$

The well-posedness of the above variational problem is proved in Appendix for a special case when  $\sigma$  is a constant.

We discretize the variational problem (2.19) using FEM, which gives Algorithm 2.

---

**Algorithm 2:** FEM with modified Nitsche's method.

---

Find  $\Phi_h \in V_{\Phi}^h$  such that for all  $v_{1,h} \in V_{\Phi,0}^h$ ,

$$a(\Phi_h, v_{1,h}) = L(v_{1,h}) \quad (2.20)$$


---

### 3. Numerical tests

In this section, we carry out numerical tests to compare the Lagrange multiplier method (Algorithm 1) with the modified Nitsche's method (Algorithm 2). We implement the two methods using FEniCS [13]. Details of the weak form implementation can be found in Appendix. In the first test,  $\sigma$  is a constant, and in the second test,  $\sigma$  is a varying function. We first show that in both cases, our proposed modified Nitsche's method in Algorithm 2 gives better accuracy. We further demonstrate that our proposed method can be solved using generalized minimal residual method (GMRES) [14] with AMG preconditioning [15].

**Test 1.** We consider a manufactured PDE in the same form as (1.1), with  $f(x, y) = -4xy + 2x$ ,  $\sigma = 1$ ,  $V = 1$ ,  $R = 1$ ,  $\Phi_D = \frac{2}{3}y^3 - y^2 + \frac{5}{6}$ ,  $\Omega = (0, 1)^2$ . This manufactured PDE has a unique solution  $\Phi_e = \frac{2}{3}xy^3 - xy^2 + \frac{5}{6}$ . The parameter  $\epsilon$  used in the modified Nitsche's method is set to  $10^{-9}$ . Numerical tests for a wide range of  $\epsilon$  are shown in Appendix.

In this test, the resulting linear systems are solved by the default direct solver using Sparse LU decomposition. For a sequence of tests, the initial mesh size is set to 0.1 and then refined by a factor of 2. For each mesh refinement, we report  $L^2$  error inside the domain,  $\|\Phi_e - \Phi_h\|_{L^2(\Omega)}$ ,  $L^2$  error on the boundary  $\Gamma_1$ ,  $\|\Phi_e - \Phi_h\|_{L^2(\Gamma_1)}$ , and  $H_0^1$  error inside the domain,  $\|\Phi_e - \Phi_h\|_{H_0^1(\Omega)}$ , i.e.  $\|\nabla(\Phi_e - \Phi_h)\|_{L^2(\Omega)}$ , where  $\Phi_e$  is the exact solution and  $\Phi_h$  is the finite element solution. The results obtained by the Lagrange multiplier method and the modified Nitsche's method are shown in Tables 1 and 2, respectively. Numerical solutions obtained by the modified Nitsche's method achieve optimal convergence rate of 2nd order under the  $L^2$  norm inside the domain. When the Lagrange multiplier method is used, the  $L^2$  error convergence rate is not optimal, although the numerical solutions still converge. As to  $L^2$  error on the boundary  $\Gamma_1$ , the modified Nitsche's method gives almost the exact solution whereas the numerical solution obtained

by the Lagrange multiplier method is much less accurate. For  $H_0^1$  error inside the domain, both methods achieve optimal convergence rate.

Mesh size	$\ \Phi_e - \Phi_h\ _{L^2(\Omega)}$	order	$\ \Phi_e - \Phi_h\ _{H_0^1(\Omega)}$	order	$\ \Phi_e - \Phi_h\ _{L^2(\Gamma_1)}$	order
0.1	$5.10 \times 10^{-3}$	*	$2.96 \times 10^{-2}$	*	$8.33 \times 10^{-3}$	*
0.05	$2.47 \times 10^{-3}$	1.04	$1.49 \times 10^{-2}$	1.00	$4.17 \times 10^{-3}$	1.00
0.025	$1.22 \times 10^{-3}$	1.02	$7.43 \times 10^{-3}$	1.00	$2.08 \times 10^{-3}$	1.00
0.0125	$6.05 \times 10^{-4}$	1.01	$3.72 \times 10^{-3}$	1.00	$1.04 \times 10^{-3}$	1.00

Table 1: Test 1 Error computation: Lagrange multiplier method with the default direct solver

Mesh size	$\ \Phi_e - \Phi_h\ _{L^2(\Omega)}$	order	$\ \Phi_e - \Phi_h\ _{H_0^1(\Omega)}$	order	$\ \Phi_e - \Phi_h\ _{L^2(\Gamma_1)}$	order
0.1	$7.35 \times 10^{-4}$	*	$2.84 \times 10^{-2}$	*	$2.01 \times 10^{-7}$	*
0.05	$1.85 \times 10^{-4}$	1.99	$1.43 \times 10^{-2}$	1.00	$9.88 \times 10^{-8}$	*
0.025	$4.63 \times 10^{-5}$	2.00	$7.13 \times 10^{-3}$	1.00	$1.89 \times 10^{-7}$	*
0.0125	$1.16 \times 10^{-5}$	2.00	$3.57 \times 10^{-3}$	1.00	$1.13 \times 10^{-7}$	*

Table 2: Test 1 Error computation: modified Nitsche's method with the default direct solver

**Test 2.** We consider another manufactured PDE, with  $f(x, y) = \sin x \cos \pi y + \pi^2 \sin x \cos \pi y$ ,  $\sigma = y + 1$ ,  $V = 1 + \frac{2}{\pi^2}$ ,  $R = 1$ ,  $\Phi_D = 1 + \sin(1) \cos \pi y$  in  $\Omega = (0, 1)^2$ . This manufactured PDE has a unique solution  $\Phi_e = \sin x \cos \pi y + 1$ . The parameter  $\epsilon$  is also set to  $10^{-9}$ . The testing results for the Lagrange multiplier method and the modified Nitsche's method are shown in Tables 3 and 4, respectively. The numerical solutions obtained by the modified Nitsche's method again achieve optimal convergence rate of 2nd order under the  $L^2$  norm inside the domain. For solutions obtained by the Lagrange multiplier method, the  $L^2$  error convergence rate is still not optimal. As to  $L^2$  error on the boundary  $\Gamma_1$ , the modified Nitsche's method also achieves 2nd order convergence rate while the Lagrange multiplier method only has 1st order convergence rate.

Mesh size	$\ \Phi_e - \Phi_h\ _{L^2(\Omega)}$	order	$\ \Phi_e - \Phi_h\ _{H_0^1(\Omega)}$	order	$\ \Phi_e - \Phi_h\ _{L^2(\Gamma_1)}$	order
0.1	$3.51 \times 10^{-2}$	*	$1.62 \times 10^{-1}$	*	$5.81 \times 10^{-2}$	*
0.05	$1.74 \times 10^{-2}$	1.01	$8.16 \times 10^{-2}$	0.99	$2.96 \times 10^{-2}$	0.97
0.025	$8.69 \times 10^{-3}$	1.00	$4.08 \times 10^{-2}$	1.00	$1.49 \times 10^{-2}$	0.99
0.0125	$4.34 \times 10^{-3}$	1.00	$2.04 \times 10^{-2}$	1.00	$7.47 \times 10^{-3}$	0.99

Table 3: Test 2 Error computation: Lagrange multiplier method with the default direct solver

Mesh size	$\ \Phi_e - \Phi_h\ _{L^2(\Omega)}$	order	$\ \Phi_e - \Phi_h\ _{H_0^1(\Omega)}$	order	$\ \Phi_e - \Phi_h\ _{L^2(\Gamma_1)}$	order
0.1	$4.85 \times 10^{-3}$	*	$1.52 \times 10^{-1}$	*	$1.91 \times 10^{-3}$	*
0.05	$1.22 \times 10^{-3}$	1.99	$7.60 \times 10^{-2}$	1.00	$4.77 \times 10^{-4}$	2.00
0.025	$3.05 \times 10^{-4}$	2.00	$3.80 \times 10^{-2}$	1.00	$1.19 \times 10^{-4}$	2.00
0.0125	$7.63 \times 10^{-5}$	2.00	$1.90 \times 10^{-2}$	1.00	$3.02 \times 10^{-5}$	1.98

Table 4: Test 2 Error computation: modified Nitsche's method with the default direct solver

We further investigate the linear solver GMRES with AMG preconditioning for solving the manufactured PDEs in both Test 1 and Test 2. We record in Tables 5 and 6 the number of iterations needed for convergence in Tests 1 and 2, respectively. The stopping criterion is when the actual residual norm is smaller than  $10^{-7}$ . It can be seen that the iterative solver GMRES with AMG preconditioning can be directly applied to the linear system resulted from the modified Nitsche's method. Moreover, the number of iterations does not increase much when the mesh is refined, which indicates the effectiveness of AMG preconditioning for the modified Nitsche's method. However, under the same settings, the Lagrange multiplier method does not converge. The ability of being solved with AMG preconditioning is also an advantage of our modified Nitsche's method over the Lagrange multiplier method, which can be crucially benefiting in addressing large scale systems.

Mesh size	Modified Nitsche's method	Lagrange multiplier method
0.1	7	Not Converge
0.05	7	Not Converge
0.025	7	Not Converge
0.0125	8	Not Converge

Table 5: Number of iterations needed using GMRES and AMG preconditioning for the PDE in Test 1

Mesh size	Modified Nitsche's method	Lagrange multiplier method
0.1	7	Not Converge
0.05	8	Not Converge
0.025	9	Not Converge
0.0125	10	Not Converge

Table 6: Number of iterations needed using GMRES and AMG preconditioning for the PDE in Test 2

#### 4. Conclusion

We derived a special integral boundary condition for the Poisson equation for a typical electric circuit model. We proposed a modified Nitsche's method to deal with the integral boundary condition and compared it with the Lagrange multiplier method. The proposed method computed the numerical solutions more accurately than the Lagrange multiplier method did, and achieved optimal convergence rate under both  $L^2$  and  $H_0^1$  norms. Moreover, iterative solvers equipped with AMG preconditioner can be directly used for solving the linear system resulted from our modified Nitsche's method, which however did not converge for the Lagrange multiplier method. The modified Nitsche's method can be useful in many physical models possessing this kind of integral boundary condition.

#### 5. Acknowledgement

This work is supported as part of the Computational Materials Sciences Program funded by the US Department of Energy, Office of Science, Basic Energy Sciences, under Award Number DE-SC0020145.

#### Appendix A. Implementation of the Lagrange multiplier method in FEniCS

The resulting variational form (2.10) can not be directly implemented using FEniCS due to the two double integrals in (2.8). Hence we introduce an auxiliary variable  $w = \int_{\Gamma_1} \sigma \frac{\partial \Phi}{\partial n} ds$  and reformulate the problem. It then becomes seeking for the stationary point of the following functional

$$\int_{\Omega} \left( \frac{1}{2} |\nabla \Phi|^2 - f \Phi \right) dx - \int_{\Gamma_1} \lambda (V - \Phi - R w) ds, \quad (\text{A.1})$$

under the constraint that

$$w = \int_{\Gamma_1} \sigma \frac{\partial \Phi}{\partial n} ds. \quad (\text{A.2})$$

Let  $V_3$  be the space of real numbers, and let  $v_3 \in V_3$  be the test function of  $w$ . The variational form consists of two parts. From (A.1), we have

$$\int_{\Omega} (\nabla \Phi \cdot \nabla v_1 - f v_1) dx + \int_{\Gamma_1} \lambda v_1 ds - \int_{\Gamma_1} v_2 (V - \Phi - R w) ds + R \int_{\Gamma_1} \lambda v_3 ds = 0 \quad (\text{A.3})$$

From (A.2), we can derive the following weak form,

$$\int_{\Gamma_1} \left( w - \int_{\Gamma_1} \sigma \frac{\partial \Phi}{\partial n} ds \right) v_3 ds = 0 \quad (\text{A.4})$$

$$\iff \int_{\Gamma_1} w v_3 ds - \int_{\Gamma_1} \sigma \frac{\partial \Phi}{\partial n} ds \int_{\Gamma_1} v_3 ds = 0 \quad (\text{A.5})$$

$$\iff \int_{\Gamma_1} \left( w - |\Gamma_1| \sigma \frac{\partial \Phi}{\partial n} \right) v_3 ds = 0, \quad (\text{A.6})$$

where  $|\Gamma_1|$  is the length of the boundary  $\Gamma_1$ .

Combining (A.3) and (A.6), we obtain the variational form in the actual implementation,

$$\int_{\Omega} \nabla \Phi \cdot \nabla v_1 dx + \int_{\Gamma_1} \lambda v_1 ds + \int_{\Gamma_1} (\Phi + R w) v_2 ds + R \int_{\Gamma_1} \lambda v_3 ds + \int_{\Gamma_1} (w - |\Gamma_1| \sigma \frac{\partial \Phi}{\partial n}) v_3 ds = \int_{\Omega} f v_1 dx + \int_{\Gamma_1} V v_2 ds \quad (\text{A.7})$$

## Appendix B. Implementation of the modified Nitsche's method in FEniCS

Due to the same reason as in the Lagrange multiplier method, in the actual implementation, we introduce an auxiliary variable  $w = \int_{\Gamma_1} \sigma \Phi ds$  for the variational form (2.19). Again we can derive the variational form for the auxiliary variable, which is

$$\int_{\Gamma_1} (w - |\Gamma_1| \sigma \Phi) v_3 ds = 0, \quad (\text{B.1})$$

Combining (2.19) and (B.1), we obtain the following variational form in the actual implementation,

$$\int_{\Omega} \nabla \Phi \cdot \nabla v_1 dx + \frac{1}{\epsilon} \int_{\Gamma_1} \left( \Phi - \frac{R}{R \int_{\Gamma_1} \sigma ds + \epsilon} w \right) v_1 ds + \int_{\Gamma_1} (w - |\Gamma_1| \sigma \Phi) v_3 ds = \quad (\text{B.2})$$

$$\int_{\Omega} f v_1 dx + \frac{1}{\epsilon} \int_{\Gamma_1} \left( V - \frac{R}{R \int_{\Gamma_1} \sigma ds + \epsilon} \int_{\Gamma_1} \sigma V ds \right) v_1 ds \quad (\text{B.3})$$

## Appendix C. Test of $\epsilon$

We look at how different choices of  $\epsilon$  affect the numerical accuracy. For this test, we use the manufactured PDE in Test 2 and compute the numerical solution on the mesh with size 0.0125.

$\epsilon$	$\ \Phi_e - \Phi_h\ _{L^2(\Omega)}$	$\ \Phi_e - \Phi_h\ _{H_0^1(\Omega)}$	$\ \Phi_e - \Phi_h\ _{L^2(\Gamma_1)}$
$10^{-2}$	$3.03 \times 10^{-3}$	$2.26 \times 10^{-2}$	$7.28 \times 10^{-3}$
$10^{-3}$	$2.88 \times 10^{-4}$	$1.90 \times 10^{-2}$	$7.40 \times 10^{-4}$
$10^{-4}$	$6.76 \times 10^{-5}$	$1.90 \times 10^{-2}$	$7.08 \times 10^{-5}$
$10^{-5}$	$7.48 \times 10^{-5}$	$1.90 \times 10^{-2}$	$2.81 \times 10^{-5}$
$10^{-6}$	$7.60 \times 10^{-5}$	$1.90 \times 10^{-2}$	$2.95 \times 10^{-5}$
$10^{-7}$	$7.62 \times 10^{-5}$	$1.90 \times 10^{-2}$	$2.98 \times 10^{-5}$
$10^{-8}$	$7.62 \times 10^{-5}$	$1.90 \times 10^{-2}$	$2.98 \times 10^{-5}$
$10^{-9}$	$7.63 \times 10^{-5}$	$1.90 \times 10^{-2}$	$3.02 \times 10^{-5}$
$10^{-10}$	$7.70 \times 10^{-5}$	$1.90 \times 10^{-2}$	$3.26 \times 10^{-5}$
$10^{-11}$	$9.66 \times 10^{-5}$	$1.90 \times 10^{-2}$	$8.61 \times 10^{-5}$
$10^{-12}$	$2.85 \times 10^{-4}$	$1.90 \times 10^{-2}$	$4.45 \times 10^{-4}$
$10^{-13}$	$3.52 \times 10^{-3}$	$2.00 \times 10^{-2}$	$6.07 \times 10^{-3}$
$10^{-14}$	$2.72 \times 10^{-2}$	$5.08 \times 10^{-2}$	$4.71 \times 10^{-2}$

Table C.1: Error computation with different epsilon values

We can see the modified Nitsche's method works for a wide range of  $\epsilon$  given a certain error tolerance. Also, as expected, the accuracy is poor with big  $\epsilon$ . This is because the modified boundary condition (2.16) becomes a poor approximation to the original integral boundary condition (1.4) when  $\epsilon$  is large. In the case when  $\epsilon$  is very small, from  $10^{-14}$  to  $10^{-11}$ , the numerical accuracy also deteriorates.

## Appendix D. Well-posedness

We prove the well-posedness of the variational problem (2.19) for a special case when  $\sigma$  is a constant.

**Theorem 1.** *Assuming that  $f \in L^2(\Omega)$ , the variational problem (2.19) for the modified Nitsche's method is well-posed for any  $\epsilon > 0$  if  $\sigma$  is a constant.*

*Proof.* Without loss of generality, we may assume  $\Phi_D = 0$ . So  $V_\Phi$  and  $V_{\Phi,0}$  are the same function space. Since  $\sigma$  is a constant, we can write the bilinear form  $a(\cdot, \cdot)$  in (2.19) as follows,

$$a(\Phi, v_1) = a_1(\Phi, v_1) + a_2(\Phi, v_1), \quad (\text{D.1})$$

where

$$\begin{aligned} a_1(\Phi, v_1) &= \int_{\Omega} \nabla \Phi \cdot \nabla v_1 dx, \\ a_2(\Phi, v_1) &= \frac{1}{\epsilon} \left( \int_{\Gamma_1} \Phi v_1 ds - \frac{R\sigma}{R \int_{\Gamma_1} \sigma ds + \epsilon} \int_{\Gamma_1} \Phi ds \int_{\Gamma_1} v_1 ds \right). \end{aligned} \quad (\text{D.2})$$

To see its boundedness property, we have

$$\begin{aligned} |a(\Phi, v_1)| &\leq \|\nabla \Phi\|_{L^2(\Omega)} \|\nabla v_1\|_{L^2(\Omega)} + \frac{1}{\epsilon} \left( \|\Phi\|_{L^2(\Gamma_1)} \|v_1\|_{L^2(\Gamma_1)} + \frac{R\sigma}{R \int_{\Gamma_1} \sigma ds + \epsilon} \|\Phi\|_{L^1(\Gamma_1)} \|v_1\|_{L^1(\Gamma_1)} \right) \\ &\leq \|\nabla \Phi\|_{H^1(\Omega)} \|\nabla v_1\|_{H^1(\Omega)} + \frac{1}{\epsilon} \left( \|\Phi\|_{L^2(\Gamma_1)} \|v_1\|_{L^2(\Gamma_1)} + \frac{R\sigma|\Gamma_1|^2}{R \int_{\Gamma_1} \sigma ds + \epsilon} \|\Phi\|_{L^2(\Gamma_1)} \|v_1\|_{L^2(\Gamma_1)} \right) \\ &\leq C_1 \|\nabla \Phi\|_{H^1(\Omega)} \|\nabla v_1\|_{H^1(\Omega)}, \text{ for some constant } C_1 \text{ and all } \Phi, v_1 \in V_\Phi, \end{aligned} \quad (\text{D.3})$$

where the last inequality follows from the trace theorem.

Knowing  $\sigma$  is a constant and applying Cauchy Schwarz inequality  $(\int_{\Gamma_1} \Phi ds)^2 \leq |\Gamma_1| \int_{\Gamma_1} \Phi^2 ds$ , where  $|\Gamma_1|$  is the length of  $\Gamma_1$ , we have

$$a_2(\Phi, \Phi) = \frac{1}{\epsilon} \left( \int_{\Gamma_1} \Phi^2 ds - \frac{R\sigma}{R \int_{\Gamma_1} \sigma ds + \epsilon} \int_{\Gamma_1} \Phi ds \int_{\Gamma_1} \Phi ds \right) \quad (\text{D.4})$$

$$\begin{aligned} &\geq \frac{1}{\epsilon} \left( 1 - \frac{R\sigma|\Gamma_1|}{R\sigma|\Gamma_1| + \epsilon} \right) \int_{\Gamma_1} \Phi^2 ds \\ &> 0. \end{aligned} \quad (\text{D.5})$$

So  $a_2(\cdot, \cdot)$  is positive definite. By Poincare inequality, we have that the bilinear form  $a_1(\cdot, \cdot)$  is strictly positive definite. Since  $a_1(\cdot, \cdot)$  is strictly positive definite and  $a_2(\cdot, \cdot)$  is positive definite, the bilinear form  $a(\cdot, \cdot)$  must be strictly positive definite.

Furthermore, following a similar argument for the bounded property of  $a(\cdot, \cdot)$ , we have

$$\begin{aligned} |L(v_1)| &\leq \|f\|_{L^2(\Omega)} \|v_1\|_{L^2(\Omega)} + \frac{1}{\epsilon} \left| V - \frac{R}{R \int_{\Gamma_1} \sigma ds + \epsilon} \int_{\Gamma_1} \sigma V ds \right| \|v_1\|_{L^1(\Gamma_1)} \\ &\leq C_2 \|v_1\|_{H^1(\Omega)}, \text{ for some constant } C_2 \text{ and all } v_1 \in V_\Phi. \end{aligned} \quad (\text{D.6})$$

This shows that  $L$  is a bounded linear functional on  $V_\Phi$ .

Therefore, the well-posedness follows from the Lax-Milgram lemma [16].  $\square$

## 6. Data Availability

The raw data required to reproduce these findings are available to download from <https://data.mendeley.com/datasets/v6h4tygkvc/1>. The processed data required to reproduce these findings are available to download from <https://data.mendeley.com/datasets/v6h4tygkvc/1>.

## References

- [1] Y. W. Lee, B.-J. Kim, J.-W. Lim, S. J. Yun, S. Choi, B.-G. Chae, G. Kim, H.-T. Kim, Metal-insulator transition-induced electrical oscillation in vanadium dioxide thin film, *Applied Physics Letters* 92 (2008) 162903.
- [2] H.-T. Kim, B.-J. Kim, S. Choi, B.-G. Chae, Y. W. Lee, T. Driscoll, M. M. Qazilbash, D. N. Basov, Electrical oscillations induced by the metal-insulator transition in vo2, *Journal of Applied Physics* 107 (2010) 023702.
- [3] N. Shukla, A. Parihar, E. Freeman, H. Paik, G. Stone, V. Narayanan, H. Wen, Z. Cai, V. Gopalan, R. Engel-Herbert, et al., Synchronized charge oscillations in correlated electron systems, *Scientific reports* 4 (2014) 4964.



- [4] Y. Shi, L.-Q. Chen, Phase-field model of insulator-to-metal transition in VO<sub>2</sub> under an electric field, *Phys. Rev. Materials* 2 (2018) 053803.
- [5] Y. Shi, L.-Q. Chen, Current-driven insulator-to-metal transition in strongly correlated vo<sub>2</sub>, *Phys. Rev. Applied* 11 (2019) 014059.
- [6] S. Kumar, J. P. Strachan, R. S. Williams, Chaotic dynamics in nanoscale NbO<sub>2</sub> mott memristors for analogue computing, *Nature* 548 (2017) 318–321.
- [7] S. Kumar, R. S. Williams, Z. Wang, Third-order nanocircuit elements for neuromorphic engineering, *Nature* 585 (2020) 518–523.
- [8] I. IBabuška, The finite element method with lagrangian multipliers, *Numerische Mathematik* 20 (1973) 179–192.
- [9] R. Glowinski, T.-W. Pan, J. Periaux, A lagrange multiplier/fictitious domain method for the dirichlet problem—generalization to some flow problems, *Japan journal of industrial and applied mathematics* 12 (1995) 87.
- [10] J. Nitsche, Über ein variationsprinzip zur lösung von dirichlet-problemen bei verwendung von teilräumen, die keinen randbedingungen unterworfen sind, *Abhandlungen aus dem Mathematischen Seminar der Universität Hamburg* 36 (1971) 9–15.
- [11] I. Babuška, The finite element method with penalty, *Mathematics of computation* 27 (1973) 221–228.
- [12] L. ELSGOLC, Chapter i - the method of variation in problems with fixed boundaries, in: L. ELSGOLC (Ed.), *Calculus of Variations*, International Series of Monographs on Pure and Applied Mathematics, Pergamon, 1961, pp. 13 – 63. URL: <http://www.sciencedirect.com/science/article/pii/B9780080095547500066>. doi:<https://doi.org/10.1016/B978-0-08-009554-7.50006-6>.
- [13] M. S. Alnæs, J. Blechta, J. Hake, A. Johansson, B. Kehlet, A. Logg, C. Richardson, J. Ring, M. E. Rognes, G. N. Wells, The fenics project version 1.5, *Archive of Numerical Software* 3 (2015).
- [14] Y. Saad, M. H. Schultz, Gmres: A generalized minimal residual algorithm for solving nonsymmetric linear systems, *SIAM Journal on Scientific and Statistical Computing* 7 (1986) 856–869.
- [15] K. Stüben, *Algebraic Multigrid (AMG): An Introduction with Applications*, GMD-Forschungszentrum Informationstechnik, 1999.
- [16] A. Bressan, *Lecture Notes on Functional Analysis: With Applications to Linear Partial Differential Equations*, Graduate studies in mathematics, American Mathematical Society, 2013. URL: <https://books.google.com/books?id=dXHQVSSfBnAC>.